Formation of 3D gratings by interferometric-mask method in $LiNbO_3$:Fe crystals

ANAHIT BADALYAN, RUBEN HOVSEPYAN, VAHRAM MEKHITARYAN, PAYTSAR MANTASHYAN*, RAFAEL DRAMPYAN
Institute for Physical Research, National Academy of Sciences of Armenia, 0203, Ashtarak-2, Armenia

3D holographic refractive gratings were created by combined interferometric-mask method in photorefractive Fe-doped lithium niobate (LN:Fe) crystal revealing high photorefractive properties. The recording of the holographic gratings were performed by 532 nm cw laser beam illumination of the crystal through 2-fold rotational symmetry mask using counter-propagating beam geometry. The gratings formed have ~30 μm period in radial and azimuthal directions and 266nm in axial direction. The gratings were tested by diffraction of red laser 633 nm Gaussian beam on the grating. The direct observation of the gratings was performed by phase microscope. Created refractive gratings are promising for many applications including guiding and trapping systems, high capacity information storage etc.

(Received June 10, 2011; accepted April 11, 2012)

Keywords: Holographic gratings, Diffraction, Photorefractive materials, Micro- and nano-structures

1. Introduction

Materials with artificial spatial periodic structures, such as the photonic crystals [1], currently find applications in many fields of physics and optical device engineering. For many applications, including guiding and trapping systems, optical devices, telecommunications, information storage etc 2D and 3D gratings are more promising. In spite of many successes in this field, the further development of the techniques for the fabrication of various photonic nano- and micro-structures is an actual problem.

Holographic technique [2] is one of the promising methods for the fabrication of spatially periodic structures in photorefractive materials. Holographic technique is based on the creation of spatially periodical structures in photosensitive materials by intensity modulated light beams. The illumination of photorefractive medium by spatially modulated beam leads to the refractive index modulation via electro-optic effect, thus creating refractive gratings. Non-uniform light beams can be created by mask technique or by beam interference arrangements.

Numerous investigations are devoted to the study of dynamic and permanent optical refractive gratings using classic two-beam interference arrangement in atomic vapors [3], crystals [4] and liquid crystals [5]. The gratings formed by two-beam arrangement are one–dimensional and have limited applications. The mask technique [6] allows the creation of 2D structures in photorefractive materials with refractive index modulation in the transverse plane. On the other hand the interferometric standing wave technique provides the intensity modulation in the axial direction. Thus the combination of mask and interferometric methods allows the creation of 3D gratings in photorefractive materials. The combined interferometric-mask method was presented in [7].

In this paper we report the formation of 3D gratings in photorefractive 0.5 mm thick LN:Fe crystal by combined interferometric - mask technique with Gaussian beams using 2-fold rotational symmetry mask.

2. Experimental set-up

For recording of 3D holographic grating, we used an experimental setup (Fig. 1) similar to that suggested in Ref. [7].

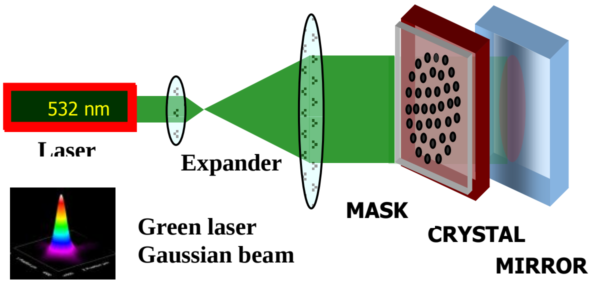

Fig. 1 (color online). Experimental setup for recording of 3D gratings by combined interferometric –mask method.

The combined interferometric–mask method is based on the illumination of the crystal through the 2D rotational symmetry masks by Gaussian beam in combination with back reflecting mirror. The counter-propagating beam geometry builds up the Gaussian standing wave, which determines the third half-wave period of the grating in the axial direction. Thus, the created 3D intensity pattern is a set of numerous mask-generated 2D quasi-periodic structures located in each anti-node of standing wave (Fig. 2).

For comparison the recording of 2D grating using only mask technique, without standing wave, was also performed.

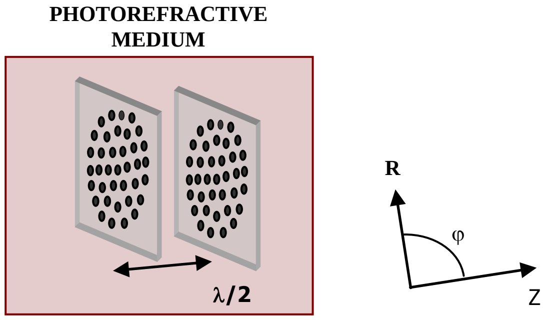

Fig. 2 (color online). Schematic of two neighboring anti-nodes of standing wave, where the mask created quasi-periodic structures are located. The grating is modulated in radial R, azimuthal φ and axial Z directions.

The mask used in the experiment had 2-fold axial symmetry and consisted of transparent holes periodically disposed along the equidistantly positioned concentric circles, surrounding the central spot (Fig. 3a). The distance between holes is about 30 μm and the total number of spots is equaled ~ 35000. The diameter of the transparent holes is about 10 μm. Fig. 3b shows the far field diffraction pattern from the mask obtained by green laser Gaussian beam.

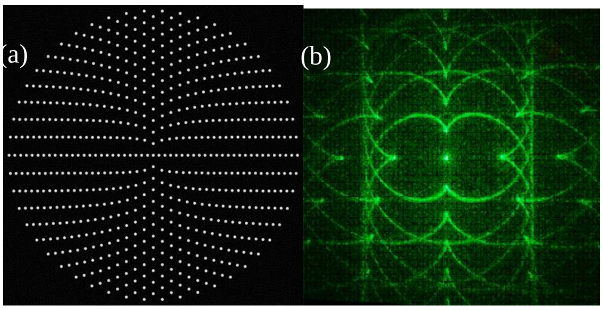

Fig. 3 (color online). (a) Fragment of enlarged pattern of 2-fold symmetry mask. (b) Far field interference pattern from 2 - fold symmetry mask obtained by green laser beam.

The laser source for recording of 2D and 3D gratings was single-mode second harmonic of cw YAG:Nd laser at 532 nm wavelength with linear polarization, 100 mW power and 1mm beam diameter. The intensity distribution of green 532 nm Gaussian beam is shown in Fig. 1. The laser beam was expanded by confocal lenses and after passing through the mask illuminated the crystal. The mask and back-reflecting mirror were practically in touch with the crystal.

The refractive index quasi-periodical structures were recorded in Y-cut 0.05 wt% LN:Fe crystal with the size of 14 × 10 ×0.5 mm^3. Optical C-axis of the crystal was oriented along the crystal surfaces. Polarization of the laser beam was directed along the C-axis of the crystal. The duration of recording was 60 min.

The gratings were tested by He-Ne cw single mode 633 nm laser Gaussian beam. The experimental scheme for the testing of the gratings is given in Fig.4.

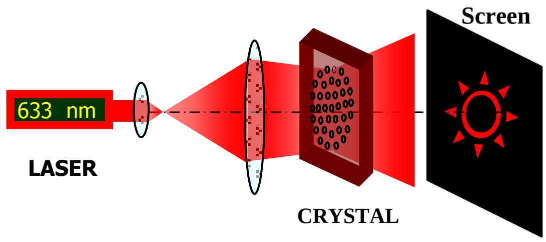

Fig. 4 (color online). Readout scheme for testing by red laser of 2D and 3D mask refractive replicas recorded inside the crystal by green laser. The screen situated in the far field shows a hypothetic diffraction pattern.

3. Results

The recorded gratings were tested using red laser beams by observing the diffraction patterns from the 2D and 3D grating in the far field. The obtained diffraction pattern from the mask refractive replica inside the crystal was compared with diffraction from the original mask. The results are shown in Fig. 5a,b.

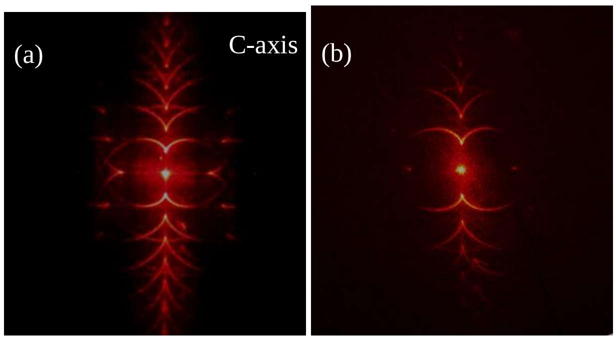

Fig.5. (color online)Diffraction patterns from 2D (a) and 3D (b) 2-fold symmetry mask refractive replica inside LN:Fe crystal.

The diffraction pattern from 2D grating (Fig.5a) showed more diffraction orders in the direction of optical C-axis of the crystal compared with diffraction from 3D gratings (Fig. 5b). It is well known, that thick holographic grating may be described as a grating exhibiting strong angular selectivity [8]. Thick grating behavior may be considered to occur when

$$d/\Lambda > 10 \quad (1)$$

where d is the thickness of the grating, Λ is the period of the grating. 3D holographic gratings recorded by combined interferometric-mask technique are thick gratings since $d/\Lambda \approx 1879 >> 10$ for d= 0.5 mm and Λ = 266 nm. Thus they exhibit strong angular selectivity and the diffraction pattern from 3D grating (thick grating) showed less diffraction orders compared with diffraction pattern from 2D grating (Fig. 5a,b).

Both gratings were recorded in 0.5 mm thick LN:Fe to minimize the diffraction effects from the holes of mask and avoid the interference effect of diffracted beams inside the crystal.

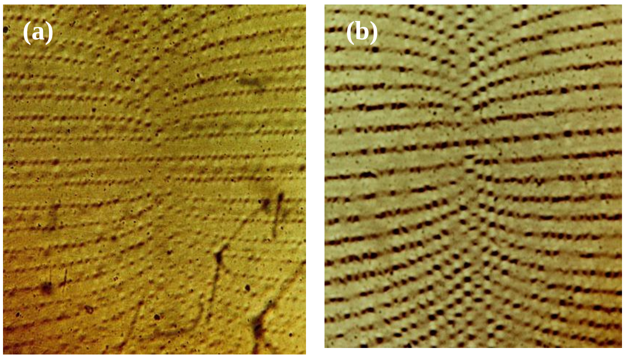

Fig.6.(color online) (a) Fragments of phase microscope image of 2D (a) and profile of 3D (b) 2-fold symmetry mask refractive replicas recorded inside 0.5 mm thick LN:Fe crystal.

Direct observation of 2D and 3D gratings recorded in LN:Fe 0.5mm thick crystal was also performed by phase microscope. The results are shown in Fig. 6a,b. 3D grating shows higher contrast than 2D gratings.

4. Discussion

The physical mechanism of formation of holographic grating in photorefractive materials is based on the electro-optic effect. Fe ions occur in LN crystal in Fe^{2+} and Fe^{3+} valence states [9]. The corresponding band diagram is shown in Fig. 7. The green light excites the electrons from Fe^{2+} to conduction band. Electrons migrate in the conduction band and finally are trapped by Fe^{3+}.

The redistribution of the charges builds up an internal electric field E and so changes the refractive index $\Delta n = RE$, where R is electro-optic coefficient. Thus, the inhomogeneous illumination of photorefractive materials leads to the modulation of refractive index. The refractive index change Δn is determined by

$$\Delta n = k_2 \, \alpha \, W \quad (2)$$

where k_2 is photorefractive sensitivity and W is energy density and α is absorption coefficient [9]. α is measured 2.6 cm^{-1} for 0.05 wt% LN:Fe crystal.

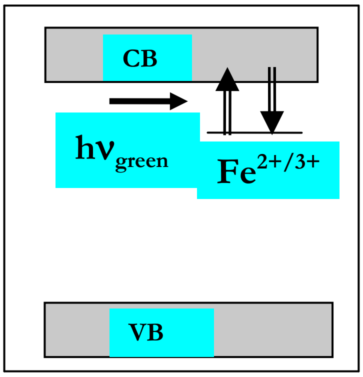

Fig. 7 (color online). Band diagram of lithium niobate doped with iron. CB is the conduction band, VB is the valence band.

As it was mentioned in Section 3 the direct observation of gratings by phase microscope showed higher contrast for 3D grating (Fig. 6). The estimation shows that the energy invested into the photorefractive LN:Fe crystal during the formation of 3D grating by combined interferometric-mask technique is about 6 times larger compared with the case of recording of 2D grating without back reflecting mirror. The cause is the multiple traversing of the beam through the crystal in the scheme with back reflecting mirror. Hence, 3D grating should have higher contrast in comparison with 2D grating (Fig. 6a,b).

5. Conclusions

3D holographic refractive gratings were formed in LN:Fe 0.5 mm thick crystals by combined interferometric–mask technique. The formed 2-fold rotational symmetry gratings have ~30 μm period in radial and azimuthal directions and 266 nm in axial direction.

The gratings were tested by probe beam. The direct observation of gratings by phase microscope was also performed.

2D and 3D gratings of different symmetry can be used as optical fibers, band-gap materials, for manipulation of beam propagation, for information storage with high capacity etc.

Acknowledgements

The authors are grateful to Dr. E Kokanyan for providing the LN:Fe crystal. The work was supported by International Science and Technology Center Grant, Project A - 1517.

References

[1] J. Joannopoulos, S. Johnson, R. Meade, J. Winn, Photonic crystals, Princeton Univ. Press, 2008.
[2] R. J. Collier, Ch. B. Buckhard, L. H. Lin, Optical holography, New York, Acad. Press, 1971.
[3] Korneev, O. Benavides, JOSA B, **25,** 1899 (2008).
[4] A. Adibi, K. Buse, D. Psaltis, JOSA B, **18**, 584 (2001).
[5] P. Pagliusi, R. Macdonald, S. Bush, G. Chipparrone, M. Kreuzer, JOSA B, **18**, 1632 (2001).
[6] Wai-Hon Lee, Progress in Optics, Editor E Wolf, XVI, North-Holland, Chapter **3**, 121 (1978).
[7] A. Badalyan, R. Hovsepyan, V. Mekhitaryan, P. Mantashyan, R. Drampyan, Proc. of SPIE (SPIE Berlingham 2011), Vol. 7998, OH (2011).
[8] T. K. Gaylord, M. G. Moharam, Appl. Optics, **20**, 3271 (1981)
[9] A. M. Glass, D. von der Linde, T. J. Negran, Appl. Phys. Lett. **25**, 233 (1974).

*Corresponding author: mantashyan@gmail.com